

Transient Recovery Voltages at the Main 132kV Line Bay GIS Circuit Breaker in a Windfarm

Arana Aristi, Ivan; Okholm, J.; Holbøll, Joachim

Published in:
European Offshore Wind Conference and Exhibition 2011

Publication date:
2011

[Link back to DTU Orbit](#)

Citation (APA):
Arana Aristi, I., Okholm, J., & Holbøll, J. (2011). Transient Recovery Voltages at the Main 132kV Line Bay GIS Circuit Breaker in a Windfarm. In European Offshore Wind Conference and Exhibition 2011: Proceedings

DTU Library

Technical Information Center of Denmark

General rights

Copyright and moral rights for the publications made accessible in the public portal are retained by the authors and/or other copyright owners and it is a condition of accessing publications that users recognise and abide by the legal requirements associated with these rights.

- Users may download and print one copy of any publication from the public portal for the purpose of private study or research.
- You may not further distribute the material or use it for any profit-making activity or commercial gain
- You may freely distribute the URL identifying the publication in the public portal

If you believe that this document breaches copyright please contact us providing details, and we will remove access to the work immediately and investigate your claim.

Transient Recovery Voltages at the Main 132kV Line Bay GIS Circuit Breaker in a Windfarm

I. Arana, J. Okholm, and J. Holboell

Abstract—This paper presents the results of investigations of the Transient Recovery Voltage (TRV) across the terminals of the main 132kV Line Bay GIS circuit breaker (GIS CB) for Walney 2, second phase of the Walney Offshore Wind Farm. Several simulations were performed where the influence of different parameters in the network was evaluated during a fault in the onshore substation. The rate of rise of recovery voltage (RRRV) and the maximum crest voltage (U_c) of the TRV across the GIS CB were compared against the standard values based on the type test results from the GIS. The investigations were performed by means of time domain simulations using the EMT software PSCAD/HVDC. Based on the results, it was concluded that the highest RRRV appears on a system without additional stray capacitances, and the highest U_c appears when the fault is a single phase to ground.

Index Terms— Faults, Transient Recovery Voltage, EMT simulations.

I. INTRODUCTION

THE transient recovery voltage (TRV) that a circuit breaker (CB) experience is the voltage across its terminals after current interruption. The TRV wave shape is determined by the operating point of the electrical network surrounding the CB prior to interruption and the characteristics of the network [1]. Since the TRV is a determining parameter for successful current interruption, CBs are normally type tested in a laboratory to withstand a standardized TRV. This standardized TRV is determined by the maximum allowed rate of rise of recovery voltage (RRRV) and a maximum crest voltage (U_c).

The work made by DONG Energy in cooperation with the Technical University of Denmark is part of ongoing efforts to improve the accuracy of electrical modelling of power system components.

II. WALNEY OFFSHORE WIND FARM

The Walney Offshore Wind Farm (WOW) project is located approximately 15km west of Barrow-in-Furness in Cumbria at the East Irish Sea. The project consists of Walney 1 (WOW1) and Walney 2 (WOW2) each with 51 3.6MW wind turbines (WTs), giving a total capacity of the Walney project of 367.2MW.

The WTs are connected in “rows” by 36kV submarine cables. Pairs of rows are then connected to the platform by one radial feeder cable. Two park transformers (120MVA YNd1 132/33kV) are placed on an offshore platform in the

centre of each wind farm. The radial feeders of half of the farm are connected to one park transformer, and the other half is connected to the other park transformer. The park transformers are connected via a single export cable system consisting of a three-phase HV submarine sea cable and a land cable to the grid connection point on land. The wind farm layout is shown in Fig. 1.

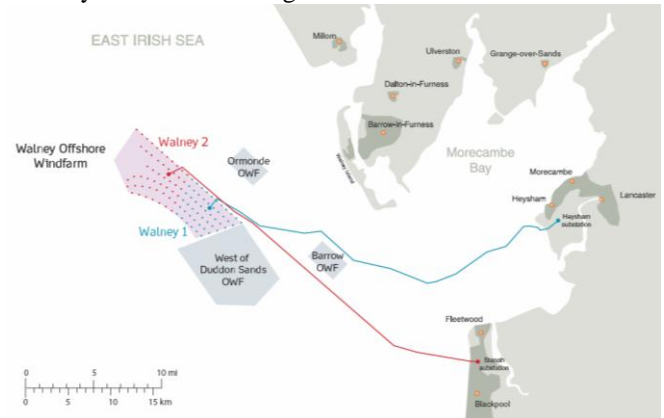


Fig. 1: Walney Offshore Wind Farm 1 + 2 layout and location

III. MODELLING THE WIND FARM

A simplified single line diagram of WOW2 with the main components included in the simulations is shown in Fig. 2.

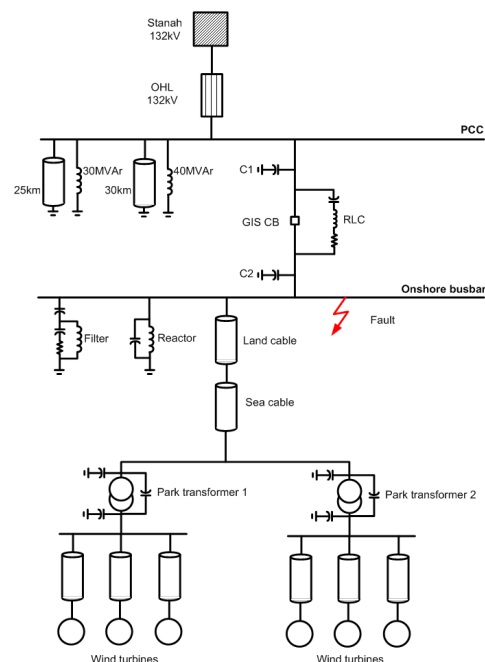


Fig. 2: Single line diagram of the external grid, export circuit and collection grid of WOW2.

I. Arana and J. Okholm are with DONG Energy, Denmark (e-mail: ivaar@dongenergy.dk and janok@dongenergy.dk, respectively)

J. Holboell is with The Technical University of Denmark, Denmark (e-mail: jh@elektro.dtu.dk)

The model of the WOW2 was created in PSCAD to predict the highest possible RRRV and U_c across the CB terminals after current interruption. In order to do so, several simulations were performed with variation of selected parameters. The different simulated faults included were

three phase ungrounded, line to line and single line to ground faults. The influence of different operating conditions on the TRV was investigated by variation of the production level of WOW2. The calculated values were compared against the standard values based on the IEC 62271-100:2008 and the type test results.

The export circuit and a simplified collection grid of WOW2 are modelled up to the point of common coupling (PCC) at 132kV level. WOW2 will connect to the Stanah substation of the United Utilities network. Each electrical component is modelled from the Onshore busbar over 132kV export circuit down to three feeders on each park transformer. The wind turbines connected to each 33kV radial feeder were represented by one aggregated model connected to the radial feeder. The connection of each aggregated model was made through a long submarine cable to account for the total capacitance of all the cables in the radial feeders.

The main data and characteristics of the individual electrical components included in the simulation model are listed below.

A. Stanah 132kV substation

For all simulations in this study, the Stanah 132kV substation at the PCC is represented as a simple Thevenin equivalent network with values based on the maximum short circuit power at the 132kV busbar and the available information about the X/R ratio, as recommended in the IEEE guidelines [2].

B. Onshore 132kV substation

The switchgear in the onshore substation of WOW2 has a rated voltage of 132kV, with SF6 insulation with a rated voltage of 145kV and Lightning impulse withstand voltage of 650kV and with three-phase encapsulation. The standard values of TRV with rated voltages of 100kV to 170kV for effectively earthed systems, according to the IEC 62271-100:2008[3], are shown in Table 1. The guaranteed U_c and RRRV from the type test results are slightly higher than the standard values from the IEC, hence the guaranteed values were used for comparison.

TABLE 1
STANDARD VALUES FROM THE IEC 62271-100:2008 USED TO COMPARE
THE RESULTS FROM PSCAD

Test	U_c [kV]	RRRV [kV/ μ s]
Terminal fault	215	2
Short line fault	166	2
Out-of-phase	295	1,54

C. Reactor and harmonic filter in onshore substation

The onshore reactor has been modelled as a simple 80MVAR reactor in parallel with a capacitance in parallel to account for the first resonance frequency obtained from the frequency response analysis (FRA) performed by the manufacturer on a similar reactor. Similar reactor equivalents have been used before [4]. The C-type filter has been modeled with four lumped elements as can be seen in fig. 2.

D. Simplified 132kV GIS CB

In the model three elements connected at the terminals of

the main 132kV GIS CB were included to account for the capacitances connected to the GIS busbar at the PCC in the Onshore substation, C1 and C2 respectively; as well as a combination of three elements in series, RLC, across the terminals of the GIS CB.

The value of C1 and C2 were based on the recommended values for a three-in-one bus capacitance per meter for systems with a rated voltage of 245 kV and below [1].

The RLC values used across the GIS terminals are similar to the ones used in [5], since no additional information was available at the time of the study.

E. Submarine cables

Some other cables, not part of the WOW2 wind farm system, such as export circuit cable and collection grid cables of other wind farms also already connected or planned to be connected at the PCC have been included in the WOW2 model. All 132kV cables were modelled as frequency dependant (phase) models based on the geometrical information provided by the manufacturer and IEEE guidelines [6]. The length of the export submarine cable is 45.1km and the export land cable is 2.63km. The other cables connected to the PCC of WOW2 are modelled based on the export submarine cable of WOW2; one of these cables has a length of 25km and another 30km. The 25km cable is compensated by a 30MVAR reactor and the 30km cable by a 40MVAR reactor.

The 33kV collection grid cables are modelled as PI sections of 150mm², each with a total length of 4.25km in order to account for five individual 0.85km cables.

F. Park transformers

The two identical transformers on the offshore platform for the export circuit are insulated with mineral oil. The transformers are modelled in PSCAD as a standard T-equivalent circuit model of a two-winding transformer based on information from the manufacturer and IEEE guidelines [7]. Neither the tap changer nor the saturation characteristic of the transformer core was included in the model.

In order to account for the capacitive coupling between windings and between each winding and ground, lumped capacitances were included; these values were obtained from FRA measurements made on the transformers [8] after the type test in the factory and again during the construction of the offshore platform.

G. Wind turbine

The wind turbines were modelled as a voltage source with inductive source impedance as in previous studies [9]. Since there are many wind turbines connected in the collection grid of WOW2, only six aggregated wind turbine models are used. This is deemed to be sufficient, given that the GIS CB connecting the export circuit to the PCC and simulated-short circuits are at 132kV in the onshore substation and not at 33kV.

H. Faults

A three phase ungrounded symmetrical fault close to the terminals of a circuit breaker will give rise to the most severe TRV across the first pole to open [1]. Similar conclusions for a 132kV circuit breaker used in onshore

TABLE 2
INFORMATION ABOUT SYSTEM CONDITION AND PARAMETER SETTING FOR EACH STUDY CASE V0 TO V12

	Stray capacitance s	Reactor	Reactor's capacitance	Filter	Wind farm production [MW/MVAr]	25km cable	30MVAr reactor	30km cable	40MVAr reactor	OHL 132kV	Fault type
V0	None	Open	Open	Open	0/0	Open	Open	Open	Open	Included	ABC
V1	C1 and RLC	Closed	Open	Open	0/0	Open	Open	Open	Open	Included	ABC
V2	C1 and RLC	Closed	Closed	Open	0/0	Open	Open	Open	Open	Included	ABC
V3	C1 and RLC	Closed	Closed	Closed	0/0	Open	Open	Open	Open	Included	ABC
V4	C1, C2 and RLC	Closed	Closed	Closed	0/0	Open	Open	Open	Open	Included	ABC
V5	C1, C2 and RLC	Closed	Closed	Closed	0/0	Closed	Open	Closed	Open	Included	ABC
V6	C1, C2 and RLC	Closed	Closed	Closed	0/0	Closed	Closed	Closed	Closed	Included	ABC
V7	C1, C2 and RLC	Closed	Closed	Closed	180/0	Closed	Closed	Closed	Closed	Included	ABC
V8	C1, C2 and RLC	Closed	Closed	Closed	180/135	Closed	Closed	Closed	Closed	Included	ABC
V9	C1, C2 and RLC	Closed	Closed	Closed	180/-135	Closed	Closed	Closed	Closed	Included	ABC
V10	None	Open	Open	Open	0/0	Open	Open	Open	Open	Not included	ABC
V11	None	Open	Open	Open	0/0	Open	Open	Open	Open	Included	A-G
V12	None	Open	Open	Open	0/0	Open	Open	Open	Open	Included	B-C

wind farms have been made in [10]. Thus, this type of fault was examined first.

The ungrounded three phase fault (ABC), the two phase (B-C) and the single phase to ground fault (A-G) were modelled using the standard fault models in PSCAD without any fault impedance. All the faults were simulated to occur at the 132kV onshore substation busbar.

IV. SIMULATION PROCEDURE

In order to evaluate the effect of different components in the export circuit and collection grid, several simulations were performed to show different TRV characteristics. The system condition and the main parameters varied for each study case as shown in Table 2.

A. Stray capacitances (V0 to V4)

Different stray capacitances are included for each study case. The 30km and 25km cables with the reactors are not included. The active and reactive power production from the entire wind farm is set to zero. Here only the 3-phase ungrounded fault is simulated (ABC).

B. Cables connected to the PCC (V5 and V6)

All the stray capacitances are included. The 30km and 25km cables with the reactors are included for each study case, respectively. The active and reactive power production from the entire wind farm is set to zero. Here only the 3-phase ungrounded fault is simulated.

C. Wind farm production (V7 to V9)

All the stray capacitances are included. The 30km and 25km cables with the reactors are included. The active and

reactive power production from the entire wind farm is varied for each study case. Here only the 3-phase ungrounded fault is simulated.

D. OHL in the external grid (V10)

No stray capacitances are included. The 30km and 25km cables with the reactors are not included. The active and reactive power production from the entire wind farm is set to zero. Here only the 3-phase ungrounded fault is simulated. Here the Overhead line (OHL) at 132kV between the PCC and the network equivalent is removed.

E. Fault type (V11 and V12)

No stray capacitances are included. The 30km and 25km cables with the reactors are not included. The active and reactive power production from the entire wind farm is set to zero. Here the 2-phase and 1-phase faults are evaluated

V. SIMULATION RESULTS

The results from all the study cases are shown in Fig. 3 to Fig. 7. Table 3 shows a summary of the maximum Uc and RRRV for the different study cases for the TRV in the GIS CB in WOW2.

Fig. 3 shows the results from the study case V0. The triggering signals for the fault and GIS CB models are shown on the first subplot. In the second subplot the currents at the PCC are shown; the third subplot shows the voltages at the PCC and the last subplot shows the voltage across the GIS CB terminals. It can be seen that the fault occurs at 0.1s and then at 0.12s the fault is cleared, and that subsequently . the first phase current that crosses zero is A, then C and finally B. The voltage across the CB shows very fast

oscillations.

Fig. 4 shows the voltage across the GIS CB terminals of phase A from the study cases V0 to V9. It can be seen that all the results can be divided in three groups: very fast RRRV ($>1\text{kV}/\mu\text{s}$) in study case V0; fast RRRV ($\approx 1\text{kV}/\mu\text{s}$) in study cases V1, V2, V3 and V4; slow RRRV ($<1\text{kV}/\mu\text{s}$) in study case V5, V6, V7, V8 and V9. Looking at table 2, it is reasonable to assume that the different RRRVs are due to the amount of capacitances connected in the external 132kV network side of the GIS CB. The worst study case is the one where no capacitances are used (V0). The voltage across the GIS CB terminals of phase B and C from the study cases V0 to V9 is very similar to Fig. 4, so these results are not shown again.

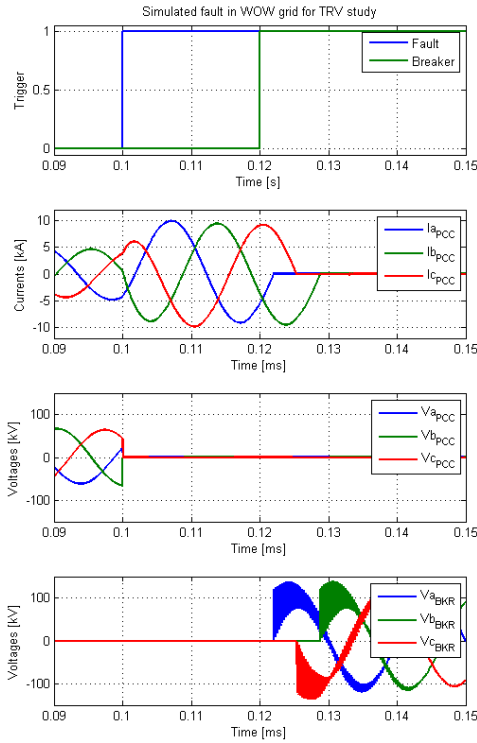


Fig. 3: Simulation results from the study case V0. The triggering signals for the fault and GIS CB models are shown on the first subplot. In the second subplot the currents at the PCC are shown; the third subplot shows the voltages at the PCC and the last subplot shows the voltage across the GIS CB terminals.

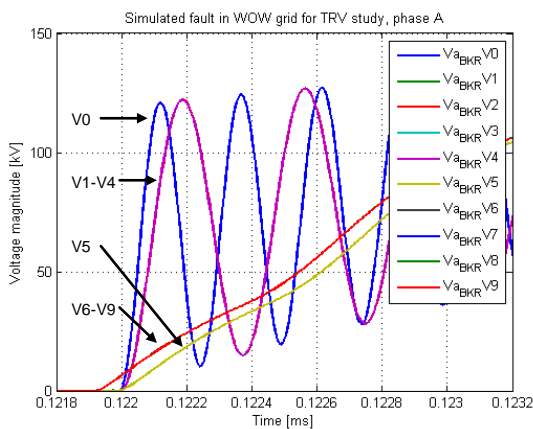


Fig. 4: Simulation results from the study cases V0 to V9. The voltage across the GIS CB terminals of phase A is shown.

Fig. 5 shows the worst TRV, found in study case V0. The voltage across the GIS CB terminals of phase A is shown as well as the withstand capabilities of the GIS CB based on

IEC values. It is possible to see that even though the maximum voltage and RRRV are very high, these values do not reach any of the standard levels of the GIS CB.

Fig. 6 shows the results from the study case V10. The triggering signals for the fault and GIS CB models are shown on the first subplot. In the second subplot the currents at the PCC are shown; the third subplot shows the voltages at the PCC and the last subplot shows the voltage across the GIS CB terminals. It can be seen that even if the short circuit current increases due to the direct connection of the GIS CB to the external 132kV network, the maximum voltage and RRRV do not reach any of the standard withstand levels of the GIS CB

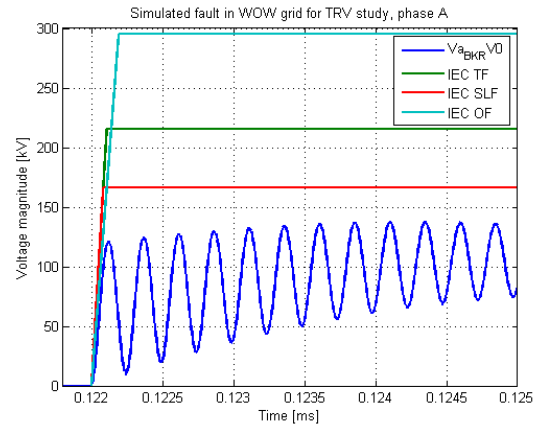


Fig. 5: Simulation results from the study case V0. The voltage across the GIS CB terminals of phase A is shown as well as the withstand capabilities of the GIS CB based on IEC values of the Uc and RRRV for terminal fault (TF), short line fault (SLF) and Out-of-phase (OF).

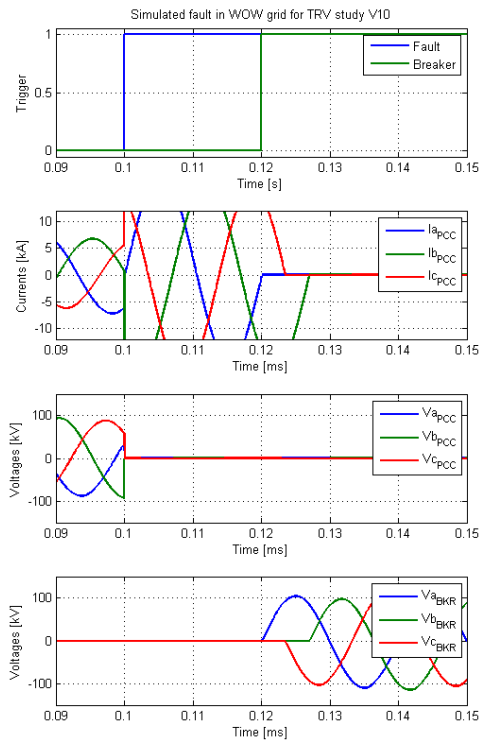


Fig. 6: Simulation results from the study case V10. The triggering signals for the fault and GIS CB models are shown on the first subplot. In the second subplot the currents at the PCC are shown; the third subplot shows the voltages at the PCC and the last subplot shows the voltage across the GIS CB terminals.

Fig. 7 shows the voltage across the GIS CB terminals of phase A, B and C for the study cases V0, V11 and V12; also

the withstand capabilities of the GIS CB based on IEC values are shown. It can be seen that the highest voltage is reached in the study case V11 on phase C. The signals from phase B and C have been shifted in time in order to compare all phases and study cases in one plot.

Table 3 shows a summary of the maximum U_c and RRRV for the different study cases for the TRV in the GIS CB in WOW2. Here, three groups of results clearly can be identified, depending on their RRRV:

- very fast RRRV ($>1\text{kV}/\mu\text{s}$) in study cases V0, V11 and V12,
- fast RRRV ($\approx 1\text{kV}/\mu\text{s}$) in study cases V1, V2, V3 and V4,
- slow RRRV ($<1\text{kV}/\mu\text{s}$) in study case V5, V6, V7, V8, V9 and V10.

By comparing the results of Fig. 4 and Fig. 7 it can be seen that the RRRV is strongly dependant on the amount of capacitances connected in the external 132kV network side of the GIS CB. While the maximum voltage U_c depends mainly on the type of fault.

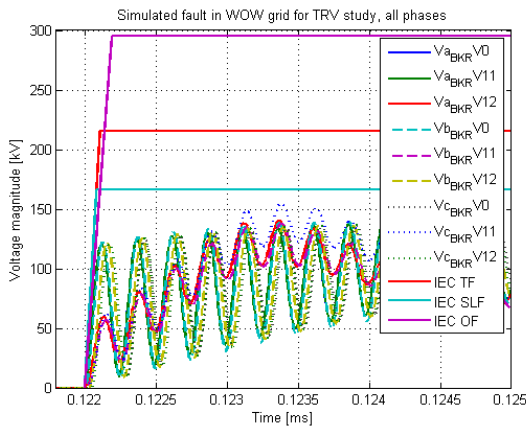


Fig. 7: Simulation results from the study case V0, V11 and V12. The voltage across the GIS CB terminals of phase A, B and C are shown as well as the withstand capabilities of the GIS CB based on IEC values of the U_c and RRRV for terminal fault (TF), short line fault (SLF) and Out-of-phase (OF).

TABLE 3
PSCAD STUDY CASE RESULTS

	Maximum U_c across the GIS CB in kV from all phases.	Maximum RRRV across the GIS CB in $\text{kV}/\mu\text{s}$ from all phases
V0	137	1.53
V1	137	1.005
V2	137	1.005
V3	137	1.005
V4	137	1.005
V5	122	0.125
V6	118	0.123
V7	118	0.123
V8	118	0.123
V9	118	0.123
V10	104	0.034
V11	150	1.512
V12	140	1.526

VI. CONCLUSIONS

This paper present an analysis of the expected worst-case transient recovery voltage (TRV) across the GIS circuit breaker, installed in the 132kV point of common coupling at

the Walney Offshore Wind Farm 2 (WOW2). These circuit breakers have been tested according to the IEC 62271-100.

Simulations showed that the TRV after current interruption, caused by a fault in the onshore substation of WOW2, would not exceed the withstand boundary defined by the TRV ratings. The lowest IEC withstand capability values of rate of rise of recovery voltage (RRRV) and the maximum crest voltage (U_c) were not reached in any of the study cases presented in this report.

It was found that the most important parameters affecting the results are the capacitances at the external 132kV network and the type of fault. The important capacitances at the external 132kV network are the GIS busbar capacitances and the capacities of other external grid cables connected at the PCC, since the capacitance at the wind farm side of the circuit breaker is already very large due to the export cable.

VII. ACKNOWLEDGMENTS

This work is made as part of an Industrial Ph.D. project supported by the Danish Ministry of Science, Technology and Innovation, project number 08-041566.

VIII. REFERENCES

- [1] "IEEE Application Guide for Transient Recovery Voltage for AC High-Voltage Circuit Breakers", IEEE Standard C37.011, Sep. 22, 2005.
- [2] IEEE PES Switching Transients Task Force 15.08.09.03, "Task Force Report, Modeling Guidelines for Switching Transients". 1997.
- [3] "High-voltage switchgear and controlgear- Part 100: High-voltage alternating-current circuit-breakers", IEC 62271-100, 2008-04.
- [4] Uglešić, I., Krepela, M., Filipović- Grčić, B., Jakl, F., "Transients Due to Switching of 400 kV Shunt Reactor" IPST 2001, Brazil.
- [5] Kondala Rao, B. and Gopal, G. Development and application of vacuum circuit breaker model in electromagnetic transient simulation. 2006. New Delhi, India: IEEE.
- [6] Gustavsen, B., Martinez, J.A., and Durbak, D., "Parameter determination for modeling system transients-Part II: Insulated cables". Power Delivery, IEEE Transactions on, 2005. **20**(3): p. 2045-2050.
- [7] Martinez, J.A., Walling, R., Mork, B.A., Martin-Arnedo, J., and Durbak, D., "Parameter determination for modeling system transients-Part III: Transformers" Power Delivery, IEEE Transactions on, 2005. **20**(3): p. 2051-2062.
- [8] Arana, I., Soerensen T., and Holboell J., "Frequency Response Variation of two Offshore Wind Park Transformers with different Tap Changer Positions" International Workshop on Large-Scale Integration of Wind Power into Power Systems as well as on Transmission Networks for Offshore Wind Farms in Quebec City, Canada, 18-19 October 2010.
- [9] Arana, I., Okholm, J., and Holboell, J., "Validation of a Switching Operation in the External Grid of Gunfleet Sand Offshore Wind Farm by Means of EMT Simulations" International Workshop on Large-Scale Integration of Wind Power into Power Systems as well as on Transmission Networks for Offshore Wind Farms in Aarhus, Denmark, 25-26 October 2011
- [10] Nanka-Bruce, O.; Nurse, S.; Jones, M.; Levi, V.; "TRV investigation to assess the suitability of 132kV circuit breaker for an offshore wind farm connection" IPST 2009, Japan.